

FINITE ELEMENT ANALYSIS OF MOISTURE AND  
THERMAL INDUCED STRESS IN  
FLIP CHIP PACKAGES

by

SANTANU GHOSH

Presented to the Faculty of the Graduate School of  
The University of Texas at Arlington in Partial Fulfillment  
of the Requirements  
for the Degree of

MASTER OF SCIENCE IN MECHANICAL ENGINEERING

THE UNIVERSITY OF TEXAS AT ARLINGTON

May 2006

Copyright © by Santanu Ghosh 2006

All Rights Reserved

To my parents

## ACKNOWLEDGEMENTS

I am very grateful to Dr Brian Dennis, my advisor, for his help and guidance in my research work. I also want to express my sincere thankfulness to Dr. B. P. Wang and Dr. Z. Han, for their support and invaluable advice for my work. I would also like to thank Dr. K. Lawrence for the clarifications and inputs I received from him whenever I went to him for clearing any doubt in ANSYS. I also express my appreciation for the staff at the MAE office who have been very friendly, efficient and co-operative. I also take this opportunity to express my respect, love and appreciation for my family for their encouragement and support. Finally a special note of thanks goes out to my sister, Dr. Rinku Majumder for her constant support, encouragement and help throughout this period.

April 18, 2006

## ABSTRACT

# FINITE ELEMENT ANALYSIS OF MOISTURE AND THERMAL INDUCED STRESS IN FLIP CHIP PACKAGES

Publication No. \_\_\_\_\_

Santanu Ghosh, MS

The University of Texas at Arlington, 2004

Supervising Professor: Dr. Brian Dennis

The process of moisture absorption and subsequent hygroswelling stress development is a cause of concern in the IC packaging industry. Also thermal stresses developed during the lead free reflow process with a high peak temperature ( $\sim 250^{\circ}\text{C}$ ) add to the problem. In Flip Chip packages, the related effects are high shear stresses at the multilayer interfaces and normal stresses in solder balls. This can lead to phenomenon like delamination at the interfaces and UBM opening. In this work we have made an attempt to simulate the moisture absorption process, subsequent hygroswelling stress development, and thermal stress generated during reflow using

established FEA techniques. A generic FC package is used as a test vehicle and the analysis is done for two different underfill materials. Also comparison is made with published results for two different test cases.

## TABLE OF CONTENTS

ACKNOWLEDGEMENTS.....	iv
ABSTRACT .....	v
LIST OF ILLUSTRATIONS.....	ix
LIST OF TABLES.....	xi
CHAPTER	
1. INTRODUCTION.....	1
1.1 Present Analysis.....	4
1.2 Result Verification.....	6
2. MOISTURE DIFFUSION ANALYSIS .....	7
2.1 Modeling.....	7
2.2 Boundary Conditions.....	10
2.3 Results.....	11
3. HYGRO-MECHANICAL STRESS ANALYSIS.....	14
3.1 Modeling.....	15
3.2 Boundary Conditions.....	17
3.3 Results.....	18
4. THERMAL STRESS ANALYSIS OF SOLDER REFLOW.....	23
4.1 Modeling.....	24
4.2 Boundary Conditions.....	25

4.3 Results.....	26
5. COMPARISON WITH PUBLISHED DATA .....	29
5.1 Modeling.....	30
5.2 Moisture Diffusion Results.....	31
5.3 Hygroscopic Stress Results.....	33
6. CONCLUSION AND FUTURE WORK.....	36
6.1 Future Work.....	37
Appendix	
A. APDL CODE FOR MOISTURE DIFFUSION (UNDERFILL A) .....	38
B. APDL CODE FOR HYGROSWELLING (UNDERFILL A) .....	45
C. APDL CODE FOR SOLDER REFLOW (UNDERFILL A) .....	48
REFERENCES .....	53
BIOGRAPHICAL INFORMATION.....	56



## LIST OF ILLUSTRATIONS

Figure	Page
1.1 Schematic of Package Evolution.....	1
1.2 Schematic of Wire bonded BGA package.....	2
1.3 Schematic of a Flip Chip BGA .....	2
1.4 2-D Half model.....	5
1.5 Meshed model .....	5
1.6 Magnified view of meshed solder balls.....	6
2.1 Discontinuous moisture concentration.....	8
2.2 Continuous wetness fraction .....	9
2.3 Boundary conditions for moisture diffusion analysis .....	11
2.4 Transient wetness distribution in package with underfill A.....	12
3.1 UBM opening and delamination during PCT.....	15
3.2 Boundary condition for hygroscopic stress model .....	17
3.3 Package deformation due to hygroscopic stress .....	18
3.4 Decreasing normal stress in solder balls (from end towards center).....	19
3.5 Normal stress in right most solder ball (magnified).....	20
3.6 Decreasing shear stress in solder balls (from end towards center).....	20
3.7 Shear stress in right most solder ball (magnified) .....	21
3.8 Comparison of maximum stress for the two packages .....	22

4.1	Boundary conditions for thermal stress .....	26
4.2	Package deformation at maximum reflow temperature.....	27
4.3	Normal stress distribution for package with underfill A .....	27
4.4	Shear stress distribution for package with underfill A .....	28
4.5	Comparison of maximum stress values for the two different underfills .....	28
5.1	Schematic of package .....	29
5.2	FEA model.....	30
5.3	Meshed model.....	30
5.4	Meshed solder balls .....	31
5.5	Transient moisture distribution for different underfill materials [3] .....	31
5.6	Moisture distribution in package with underfill A (left) and underfill C (right) .....	32
5.7	Results of parametric studies on hygroswelling stress [3].....	33
5.8	Normal stress ( $S_y$ ) distribution in solder with maximum stress (control case) .....	34
5.9	Structural energy error estimation for the solder (control case).....	34
5.10	Comparison of stress values between published values and present analysis.....	35

## LIST OF TABLES

Table	Page
2.1 Variable Mapping.....	8
2.2 Moisture properties of underfill and BT substrate .....	9
3.1 Values of $\beta$ .....	17
4.1 Comparison of eutectic SnPb soldering parameters and SnCuAg lead-free soldering parameters.....	24
4.2 Thermo-mechanical material properties.....	25

## CHAPTER 1

### INTRODUCTION

Modern day requirement for high density packaging has led to a reduction in the package size. The main requirement is to have a greater number of I/O in a smaller area. This has led to the transition from peripheral packages to area array packages as shown in the schematic below. [5]

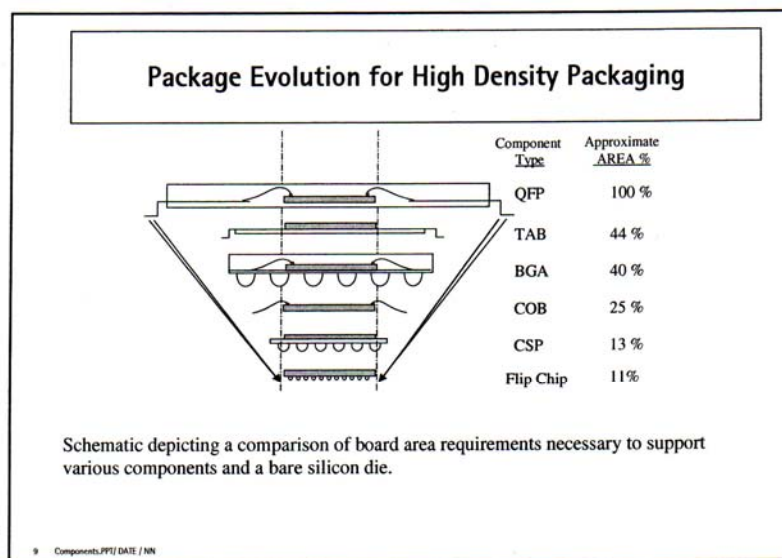


Figure 1.1: Schematic of Package Evolution

Examples of such area array packages are Ball Grid Array (BGA), Flip Chip (FC) and Chip Scale packages (CSP). Here the package to board interconnection is achieved by an area array of solder balls or columns using surface mount technology. This method of interconnection is generally used for package to board attachment.

However the same method can also be used for forming interconnection between die and the substrate, which is a part of the package. This replaces the more conventional method of wire bonding, and is used in Flip Chip BGA packages. Shown below are typical schematic cross-section for wire bonded and Flip Chip BGA packages. [6, 9]

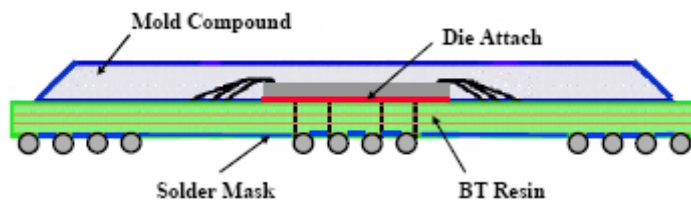


Figure 1.2: Schematic of Wire bonded BGA package

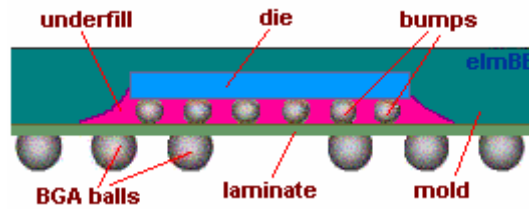


Figure 1.3: Schematic of a Flip Chip BGA

There is strong advantage gained in this by effectively using the area of the die to form interconnections. This greatly reduces the package size wherein package dimensions are closer to die dimensions. However, there is a price to pay due to,

1. Low 'flexibility' of solder balls compared to wire bonds, [8]
2. Coefficients of thermal expansion mismatch between substrate and die.

Such interconnections are not good when subjected to thermal loading, such as the solder reflow process. It also has a poor fatigue life under thermal cyclic loading and is possibly not good for shock loads.

One way to improve the performance of such packages to thermal loading (cyclic/non-cyclic) is to have an epoxy underfill between the die and BT substrate, in the space between the solder balls. This underfill then acts as a thermal stress absorber around the solder balls, thereby reducing stress on the solder joints and improving fatigue life. [14]

The problem with this is that most underfill materials have a tendency to absorb moisture during pre conditioning/storage. This leads to development of

1. Hygroscopic stress: The hygroscopic, hygroswelling or hygro-mechanical stress develops due to the CME (co-efficient of moisture expansion) mismatch between underfill, solder and die and is similar to thermal stresses that develop due to CTE mismatch. [3]

2. High vapor pressure induced stress: At high temperatures during the process of solder reflow, the entrapped moisture within the package attains high pressure and induces high local stresses within the package. [13]

The possible effects of such stresses are delamination around the die-underfill interface or opening of solder ball-die joint (UBM opening), especially at higher temperatures.

## 1.1 Present Analysis

In this work we take a look at the following,

1. Moisture diffusion: The transient moisture distribution is analyzed using the wetness thermal analogy. This is a well established technique as outlined by E.H. Wong et al [2]. It uses the Fick's diffusion equation wherein a new quantity wetness-fraction, 'w' is defined and used in place of concentration. The continuous nature of this parameter at material interfaces can be proved using a partial pressure approach. [1] The saturation time for the package depends on the moisture diffusivity of the materials whereas the final moisture level is related to the parameter saturated moisture concentration.

2. Resulting Hygroscopic Stress: This is simulated as a thermo-mechanical analysis with the parameter 'w' replacing temperature. Changes are also done for the parameter thermal co-efficient of expansion, and are discussed in detail later. The hygromechanical stress is determined using the distribution of moisture (wetness fraction) as a load to determine the transient hygroscopic stresses in the package. The magnitude of such stresses is directly dependant on the CME of the underfill material and its saturation moisture content.

3. Thermal stress generated during reflow: Linear thermal stress modeling is done for the solder reflow process. This process is even more critical in modern day fabrication of surface mounted electronic packages because of the shift towards Lead free solders. Such solders, like SnCuAg, have high peak temperature during reflow

compared to eutectic Sn-Pb solder. Thus relatively higher stresses are generated in such cases than with eutectic lead-tin solder.

Use of FEA methods is well established in the analysis of such phenomenon. In the present analysis, the commercial FEA software ANSYS ® has been used. The analysis is done for a generic FC package and two different underfill materials. A single, 2-D half model is used for the different analysis. The mesh used is made using plane stress quadrilateral (8 node) elements and MESH 200 elements. Only boundary conditions and loadings are changed according to the nature of the analysis without any changes to the mesh. As the same mesh is used for the different simulations, care is taken that the mesh is suitable for all cases. To illustrate,

1. The mesh is dense around the interfaces but relatively less dense away from them.
2. The mesh is denser in the upper corners of the solder balls than at other areas as these regions are expected to have high stresses.

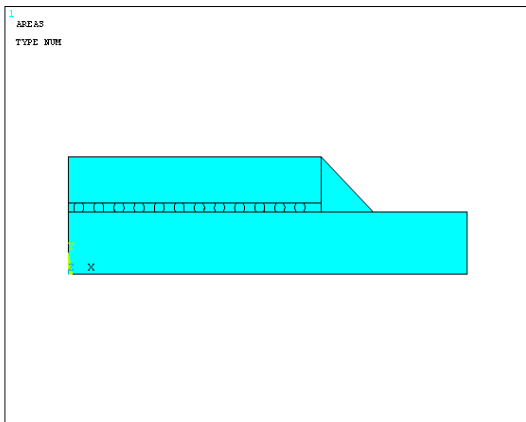


Figure 1.4: 2-D Half model

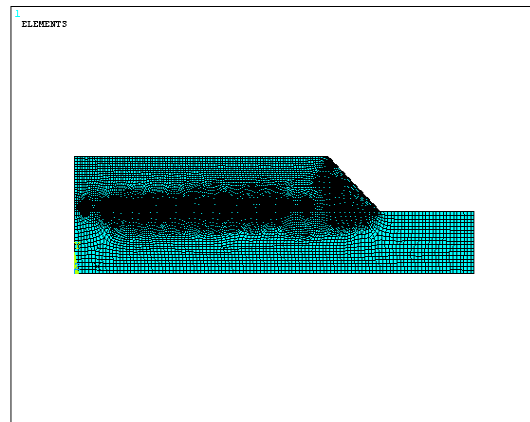


Figure 1.5: Meshed model



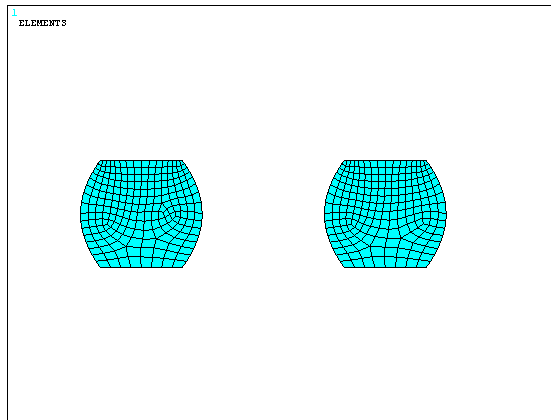


Figure 1.6: Magnified view of meshed solder balls

## 1.2 Result Verification

To establish the validity of the results, comparison is done with published data [3] for an 8x8 mm FCBGA package. The transient wetness distribution, time to saturation and the hygro-mechanical stress values at saturation are compared for two test cases. The results are discussed in detail in Chapter 5.

## CHAPTER 2

### MOISTURE DIFFUSION ANALYSIS

In FC packages, moisture is mainly absorbed by the organic layers of the BT substrate and the underfill material. The moisture diffusion occurs generally during the storage of such packages, before they are fabricated on the PWB. The degree of saturation primarily depends on the moisture diffusivity of the underfill material, other parameters remaining same. One way to determine the moisture sensitivity of the package is to do experimental testing. These tests are generally costly and require sufficient amount of time. Examples of such tests are the JEDEC Level I, (168 hrs at 85%RH/85°C) preconditioning, which give an idea of the affinity of the package to absorb moisture. An alternative, simple and non-destructive (but possibly not as effective) way to simulate such processes is to use commercial FEA software like ANSYS. FEA methods, compared to experiments, are also cost and time effective.

#### 2.1 Modeling

The process of moisture ingress is actually similar to the transient heat conduction, which is governed by the equation,

$$\partial T / \partial t = k / \rho C * \text{div} (T), \quad (2.1)$$

where,

T = temperature,

k = thermal conductivity,

$\rho$  = density,

$C$  = specific heat

The above equation is applicable for the moisture diffusion process with only a variable mapping as outlined by Wong et. al. [2].

Table 2.1: Variable Mapping

Properties	Thermal	Moisture
<i>Field variable</i>	Temperature, T	Wetness, w
<i>Density</i>	$\rho$ (kg/m <sup>3</sup> )	1
<i>Conductivity</i>	k (W/m °C)	$D * C_{sat}$ (kg/sec m)
<i>Specific capacity</i>	c (J/kg °C)	$C_{sat}$ (kg/m <sup>3</sup> )

Though, the moisture concentration ( $C$ ) can be directly substituted in equation 2.1 for temperature ( $T$ ), it is not done so. This is because the quantity moisture concentration, unlike temperature is not continuous across interfaces as shown below.

[1]

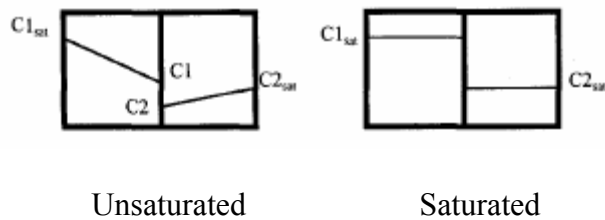


Figure 2.1: Discontinuous moisture concentration

However, the quantity wetness ( $w$ ) is continuous across interfaces [1], and is defined as

$$w = C/C_{sat} \tag{2.2}$$

where,

$C_{sat}$  = saturation moisture concentration.

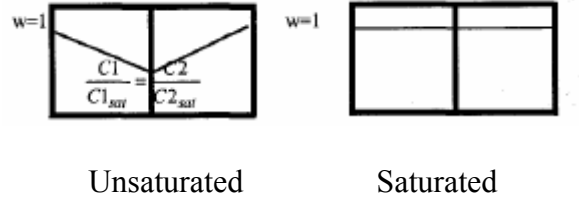


Figure 2.2: Continuous wetness fraction

The value of the properties, moisture diffusivity and  $C_{sat}$  are evaluated by experimental procedure, like moisture gain data of thin disc specimen. In the present analysis, published data [3] is used for the moisture properties of the underfill materials and the BT substrate, and is listed below.

Table 2.2: Moisture properties of underfill and BT substrate

Materials	D (mm <sup>2</sup> /s)	$C_{sat}$ (mg/mm <sup>3</sup> )
Underfill A	9.02e6	0.0152
Underfill C	1.14e5	0.0112
BT Substrate	2.13e6	0.0075

The value of the moisture properties for the non-permeable materials like solder and die are zero. However the FEM analysis of the entire package using any software requires non zero values of the same to have non-singular stiffness matrix. One way to handle this is to have very small, non-zero values of such properties. However the

problem encountered in this is that it causes a small amount of moisture diffusion across the non-permeable surfaces and is somewhat unrealistic.

In this work, to counteract this difficulty, the use of MESH 200 elements has been made. This gives a twofold advantage,

1. The moisture diffusion analysis does not involve elements which are impervious to moisture. So the problem of diffusion across non-permeable surfaces does not arise.
2. Once the moisture diffusion analysis is done, the same mesh (with solder balls and die) can be used for the hygroscopic stress analysis, using the wetness loads from the moisture diffusion solution. This only requires a proper element switching, which is done during the preprocessing of the stress analysis.

## 2.2 Boundary Conditions

The use of MESH 200 elements for the solder balls and die introduces new boundaries at the interfaces. This happens as these components are not selected for the solution procedure. The boundary conditions for these are of the normal kind, i.e. insulated, since moisture is not supposed to flow across them. One way to do it would be to select the new formed boundaries and specify a zero HFLUX on them. However a simpler way to do this is to enforce no artificial boundary conditions, since this will imply insulated boundaries. This second and more elegant method is followed here. The boundary conditions on the remaining boundaries are as follows,

1. Insulated boundary at  $x=0$ , which is the axis of symmetry. Here again no condition is specified as it would be formulated as insulated.

2. The remaining external boundaries are provided with a Dirichlet condition. A value of  $w=1$  is provided which implies ambient moisture saturation.

The initial condition is given as  $w=0$ , implying a completely dry package at  $t=0$ .

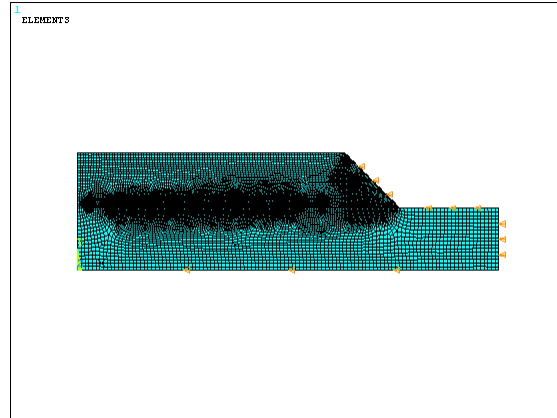


Figure 2.3: Boundary conditions for moisture diffusion analysis

### 2.3 Results

Plots of wetness distribution are done at different times and shown below for one of the two underfill materials (Underfill A).

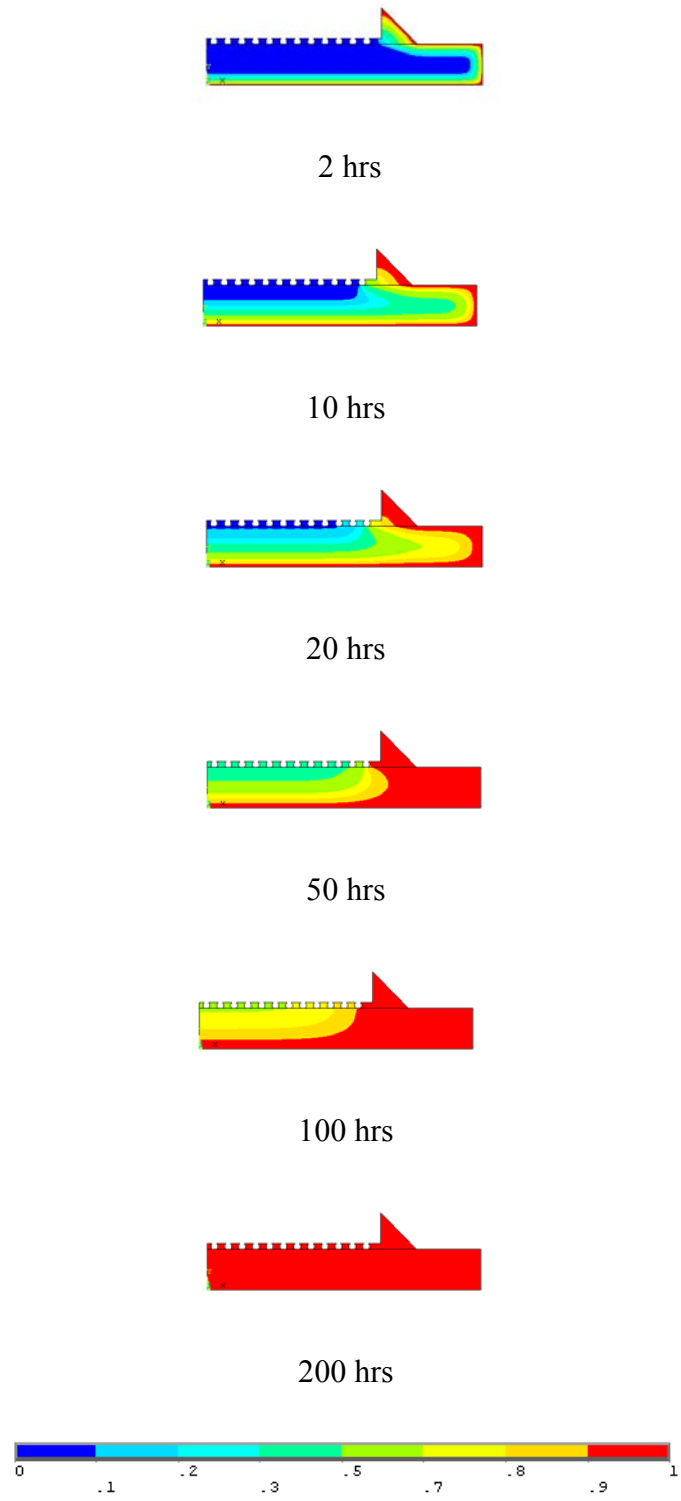


Figure 2.4: Transient wetness distribution in package with underfill A

The plots shown above do not include the solder balls and the die. This is because the MESH 200 elements are not included in the post processing of ANSYS. The saturation time for Underfill A, as shown in the figure is around 200 hrs. The same for the Underfill C is around is around 175 hrs. The package with underfill C saturates faster owing to the higher diffusivity of its underfill. The large amount of time required for saturation of these packages is mainly due to their bigger size and due to a higher number of solder balls. It will be an interesting study to note the saturation time(s) for the same package but with different numbers of solder balls.



## CHAPTER 3

### HYGRO-MECHANICAL STRESS ANALYSIS

The process of moisture ingress in the BT layers and underfill of FCBGA packages is detrimental for package performance, mainly at high temperatures as encountered during the reflow process. The harmful effects of moisture absorption are many and listed point wise below,

1. The presence of moisture along the die-underfill interface weakens the interfacial bonding and can lead to delamination.
2. Shear stresses are induced due to hygro-mechanical forces and act along the die-underfill interface. This additional factor also contributes towards die-underfill delamination.
3. At the high temperature encountered during reflow process the moisture entrapped in the package vaporizes and creates pockets of high vapor pressure. This pressure adds up with the thermal stress generated during reflow and is one of the possible causes for the “popcorn” failure in such packages. [16]
4. Tensile stress induced due to hygro-mechanical forces act on the UBM (Underside Bump Metallurgy) and may lead to UBM opening failures.

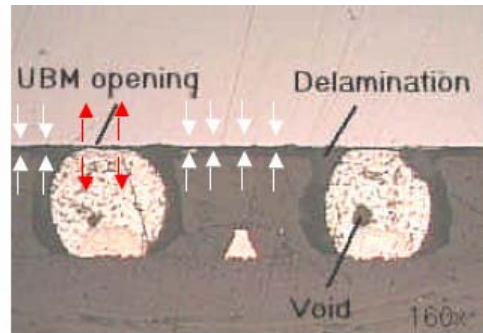


Figure 3.1: UBM opening and delamination during PCT [3]

One of most common tests done to determine package resistance to high temperature and humidity stresses is the PCT (Pressure Cooker test). PCT (121°C/100%RH, 168 hours) is a stringent accelerated test for moisture-sensitive package, especially with underfill material. FEA provides an alternative, simple and relatively inexpensive method for determining the order of magnitude and distribution of such stresses. The difficulty in such modeling is that the moisture related properties of the underfill and mold compound are difficult to ascertain at the high temperatures encountered in practical situations. So properties measured at 85° C are used to get a measure of such stresses. Thus the results obtained are only indicative, and the actual stress values in the real situation are generally much higher.

### 3.1 Modeling

CME is a measure of the change in the material strain with change in the moisture concentration. For the present work it is the measure of the materials expansion by absorbing moisture. In concept it is similar  $\alpha$ , the coefficient of thermal expansion (CTE). Thus as thermal stresses are generated due to CTE mismatch among materials, likewise hygro-mechanical stresses are induced due to CME mismatch

among different material components of the package. The general hygroswelling characterization technique has been developed by Wong et. al. [16]. According to this the hygroswelling strain can be related to CME and the local moisture concentration using the equation,

$$\varepsilon_h = \beta * C \quad (3.1)$$

Where,

$\varepsilon_h$  = hygroswelling strain,

$\beta$  = coefficient of moisture expansion (CME),

C = moisture concentration

Also, the concentration 'C' and the wetness 'w' are related by the equation,

$$C = w * C_{sat}, \quad (3.2)$$

Where,

w = wetness fraction,

$C_{sat}$  = saturated moisture concentration.

Thus using equation 3.2, equation 3.1 can be re-written as,

$$\varepsilon_h = \beta * C_{sat} * w \quad (3.3)$$

The above relation is very similar to the thermal strain equation with the quantity  $\beta * C_{sat}$  replacing  $\alpha$ . Thus the above equation can be used to find out the hygroscopic stress for a given wetness distribution. This is exactly done in the present analysis, which is treated as a thermo-mechanical problem with the wetness distribution replacing a temperature load. The average values of  $\beta$  are generally determined from

experimental data for thin disc specimen. For the present analysis published data [3] is used and is tabulated below;

Table 3.1: Values of  $\beta$

Materials	CME $\beta$	Hygro Strain $CME * C_{sat}$
Underfill A	0.18	0.0027
Underfill C	0.31	0.0035
BT Substrate	0.4	0.0030

### 3.2 Boundary Conditions

For this thermo-mechanical analysis, temperature (wetness) loads are read from the .rth file generated during the moisture diffusion analysis. There are no external mechanical forces acting, but the system is constrained as follows,

1. The boundary at  $x=0$  is an axis of symmetry for this 2-D half model. So it has symmetric boundary conditions.
2. The node at  $x=0, y=0$  is restrained.

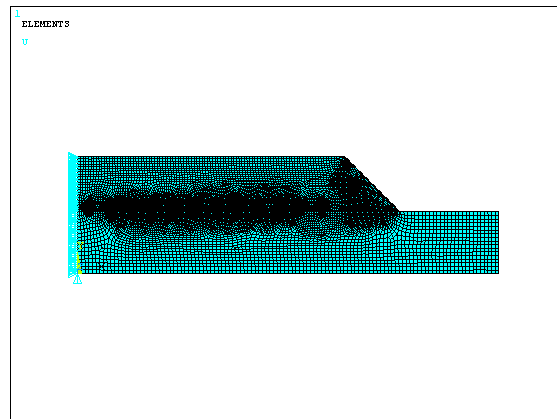


Figure 3.2: Boundary condition for hygroscopic stress model

The MESH 200 elements which had been used during the mesh generation of the diffusion modeling are now changed to plane strain 8-node quadrilateral elements. They are now included in the solution domain and as such there is no need for any boundary conditions along the interfaces as in the diffusion modeling. However, since the .rth file from the diffusion analysis does not contain the temperature for these additional nodes, they are assigned a zero value by the program. But it is not a problem. This is because the reference temperature for the thermal stress calculation is 0, which essentially implies a dry material ( $w=0$ ) and is hence desirable for the die and solder balls.

### 3.3 Results

The deformation of the package as a result of the hygroscopic stresses is shown below. The dotted line represents the undeformed package outline.

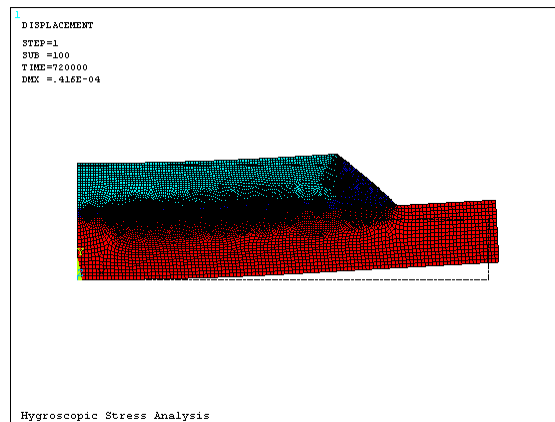


Figure 3.3: Package deformation due to hygroscopic stress

As stated earlier, the most harmful stresses induced due to moisture ingress are the shear and the normal tensile stresses acting at the interfaces. The magnitude of these

stresses are generally dependant on the quantity  $\beta \cdot C_{\text{sat}}$  of the underfill, other factors remaining unchanged. Thus the maximum stress values for the package with Underfill C are slightly higher than the one with Underfill A.

The maximum normal stress ( $S_y$ ) occurs in the right most solder ball. The values gradually decrease as we move from the end to the center of the package. Within the solder ball, the maximum state of stress occurs at the upper left corner. Shown below are normal stresses in the solder balls at saturation for package with underfill A.

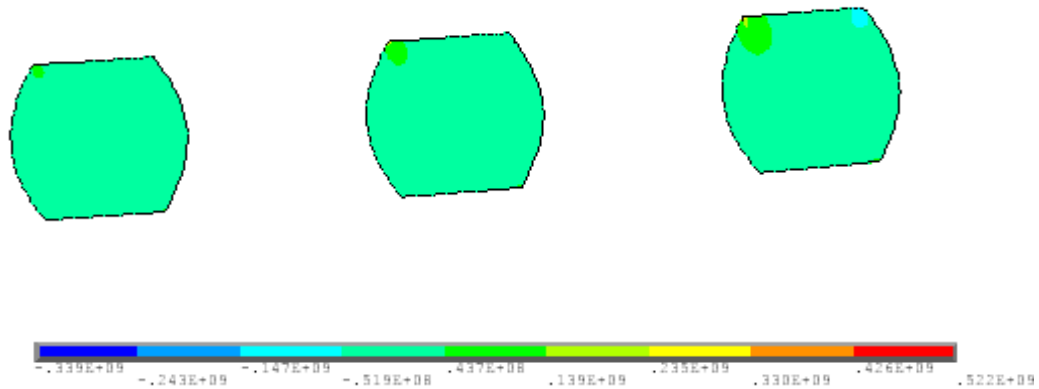


Figure 3.4: Decreasing normal stress in solder balls (from end towards center)

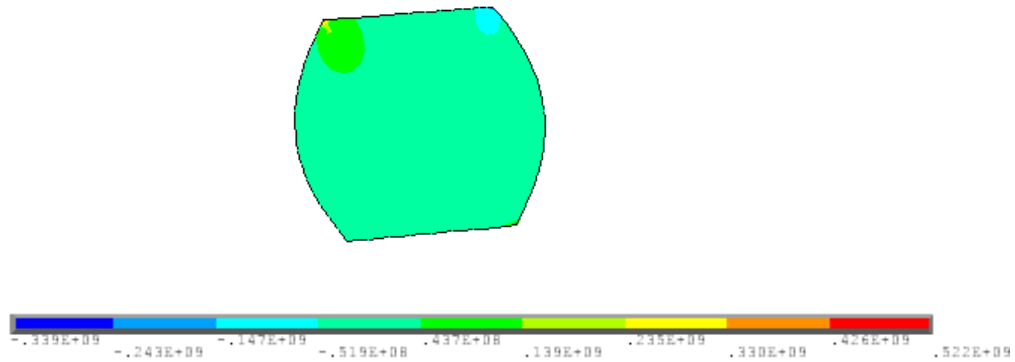


Figure 3.5: Normal stress in right most solder ball (magnified)

Similar results are obtained for the shear stress distribution in the package. Here also the maximum shear stress occurs in the solder ball nearest to the package end and values gradually decrease as we move towards the centre. Within the solder, the upper left and lower right interfaces with the underfill are under maximum shear as shown below (at package saturation).

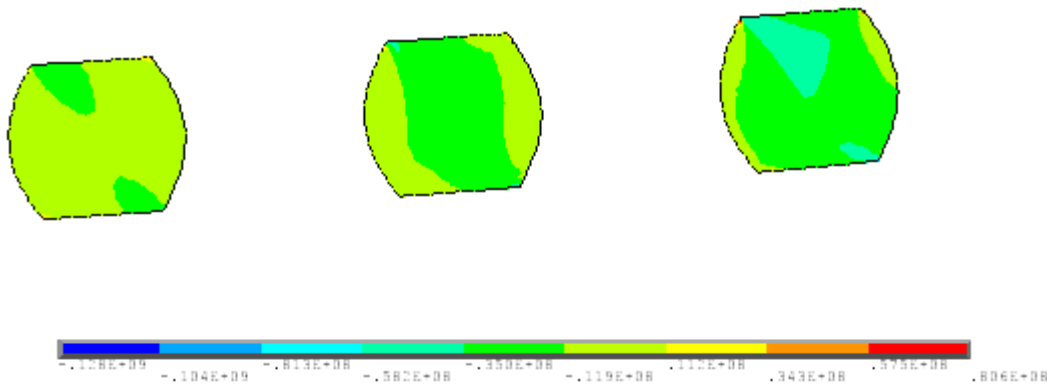


Figure 3.6: Decreasing shear stress in solder balls (from end towards center)

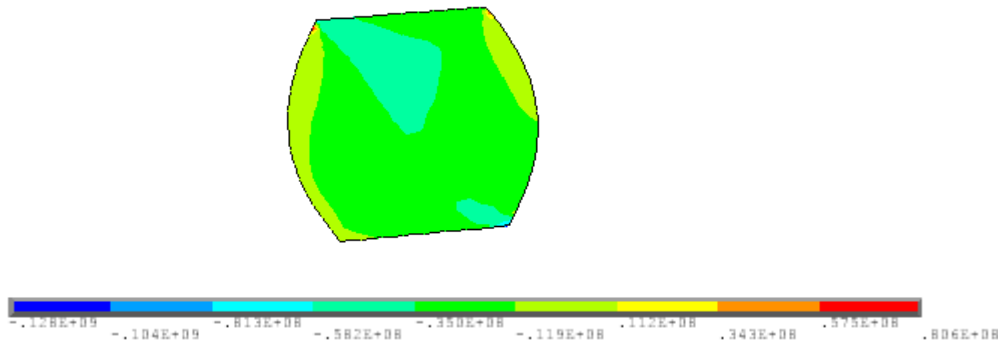


Figure 3.7: Shear stress in right most solder ball (magnified)

These results illustrate, like in the case of thermal loading, the maximum stresses are encountered in the solder ball farthest from the centre of the package. [8] These stresses are generally responsible for the separation at interfaces as encountered in such packages.

Similar results are obtained for the package stresses using underfill C. A comparative plot is done to show the relative value of the maximum normal and shear stresses for the two cases.



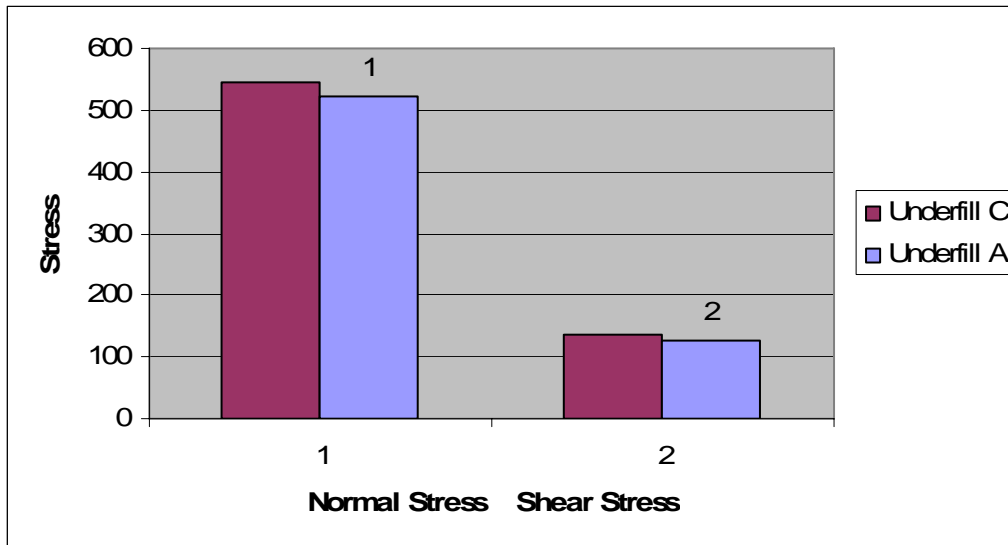


Figure 3.8: Comparison of maximum stress for the two packages

As expected, the maximum stress values for the package with underfill C is higher than in the package with underfill A.

## CHAPTER 4

### THERMAL STRESS ANALYSIS OF SOLDER REFLOW

Thermal stresses are induced in electronic packages during various stages of their lifecycle. They can be due to manufacturing processes like solder reflow, or thermal fluctuations during storage/shipping or heat generation during use. Of these, the magnitude of the stress generated during the solder reflow process is very high, and the same, in conjunction with vapor pressure often lead to package failure during the production phase. The shift in the electronic packaging industry towards Lead free assembly methods due to environmental concerns has also contributed to this. This is because the peak reflow temperatures for lead free solder alloys are generally higher (~250 ° C) than that for eutectic Pb-Sn solder (~220 ° C) [4]. A comparison of reflow profile between eutectic Pb-Sn solder vs. Lead free solder is shown in the table below.

[4]

Table 4.1: Comparison of eutectic SnPb soldering parameters and SnCuAg lead-free soldering parameters

Condition	Existing J Standard 020 A	Lead-free Soldering
Average ramp up rate to melting point	3°C/sec (max)	2.5 – 3°C/sec (max)
Pre-heat dwell time and temperature	60-120 sec (max) at 125°C (+/-0 25°C)	60-120 sec (max) at 125°C (+/-0 25°C)
Time above melting point	60-150 sec	80 sec
Time within 5oC of actual peak	10-20 sec	10-20 sec
Peak temperature range	220°C (+5/-0 C)	255°C (+5/-0 C)
Ramp down rate	6°C/sec (max)	6°C/sec (max)
Time from 25oC to peak temperature	4 min- 6 min	6 min (max)

#### 4.1 Modeling

In FCBGA package the reflow process induces high tensile stresses in the solder-die interface which contribute to the phenomenon like UBM opening and solder cracking. It is relatively simple to model this process using FEA packages like ANSYS, assuming elastic behavior of both solder and underfill. Since the nature of the underfill before curing is highly non-elastic, such analysis is done here from the post curing temperature (~165 ° C) to the reflow temperature. This is quite acceptable since for snap cure underfill packages, the curing of the underfill generally happens during the solder reflow process itself. This eliminates the need of a separate curing process for the underfill and saves on post curing time. The values of the mechanical and thermal properties for underfill and solder can be made temperature dependant which makes the problem realistic but more complicated due to non-linearity introduced. In this work we

have done linear elastic modeling with constant properties for both underfill and solder. Thermo-mechanical properties used for the different materials are listed below. [3]

Table 4.2: Thermo-mechanical material properties

Materials	Mean CTE (ppm/°C)	E at 25°C (GPa)
Silicon Die	2.6	155
BT Substrate	15	21
Underfill A	145	2.4
Underfill C	108	2.7
Solder [12] Sn-0.7Cu3.6Ag	18.8	42

A static analysis is done with a starting temperature of around 165°C, which is assumed as the curing temperature. A stress free state is assumed at the curing temperature and this is used as the reference temperature for the thermal strain calculations. The advantage of such a modeling is that if a separate non-linear visco-elastic analysis is done for the curing process, the final stress state from that can be read onto this model. It could then be considered as an initial stress state for the elastic modeling from the cure temperature to the peak reflow temperature. This would then enable the evaluation of comprehensive stresses during the reflow process using partly in-elastic and partly elastic material behavior for the different temperature zones.

#### 4.2 Boundary Conditions

The boundary conditions are same as in the hygroscopic stress analysis with  $x=0$  being an axis of symmetry and the node at  $x=0, y=0$  constrained. For applying the temperature load, all elements are selected and assigned a uniform temperature as a body load.

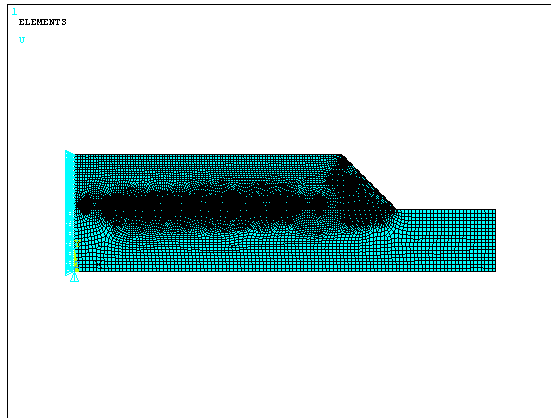


Figure 4.1: Boundary conditions for thermal stress

### 4.3 Results

During the reflow process, the maximum stress state occurs in the package at the peak temperature of reflow. For the lead free assembly process this temperature is around 30 °C higher than for conventional eutectic Pb-Sn solder reflow. This results in higher stress values for this process. As in the hygroswelling stress, the package warps in the upper direction at the maximum reflow temperature. In this case there is a pronounced swelling of the underfill due to its high value of thermal expansion coefficient.

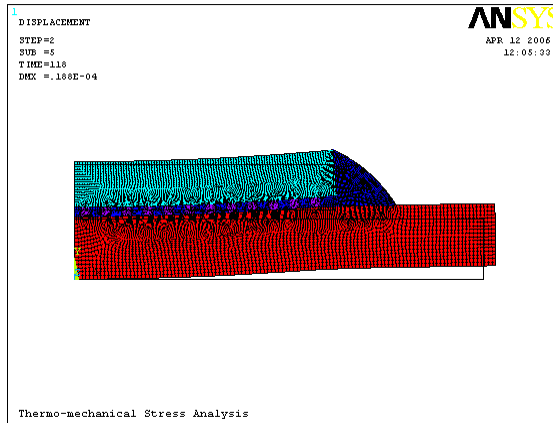


Figure 4.2: Package deformation at maximum reflow temperature

Also, the maximum normal and shear stresses act on the solder closest to the edge of the package. The plots of the same are shown here for the package with underfill A.

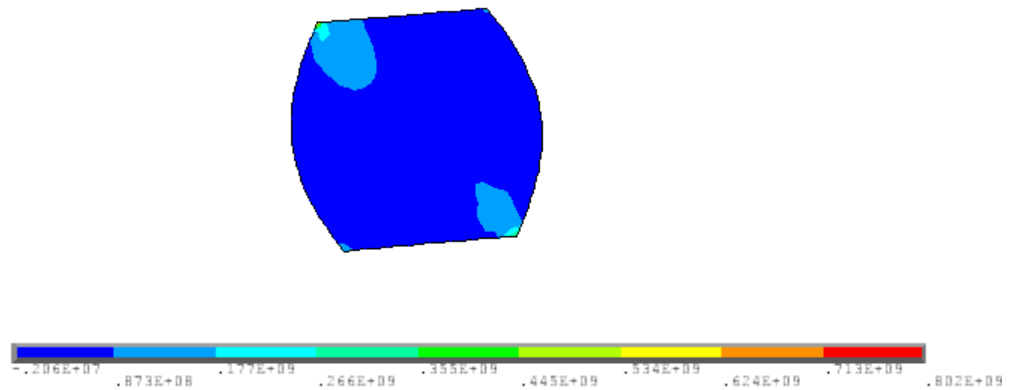


Figure 4.3: Normal stress distribution for package with underfill A

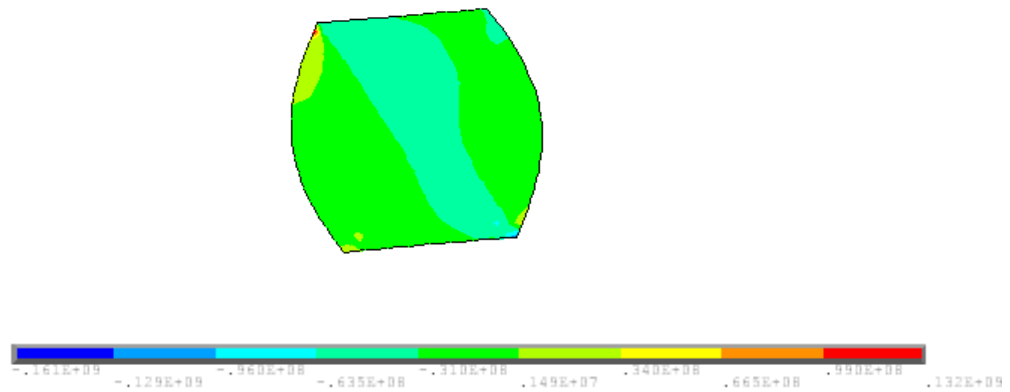


Figure 4.4: Shear stress distribution for package with underfill A

As shown here, the nature of stress distribution for the reflow process is quite similar to that due the hygroswelling process.

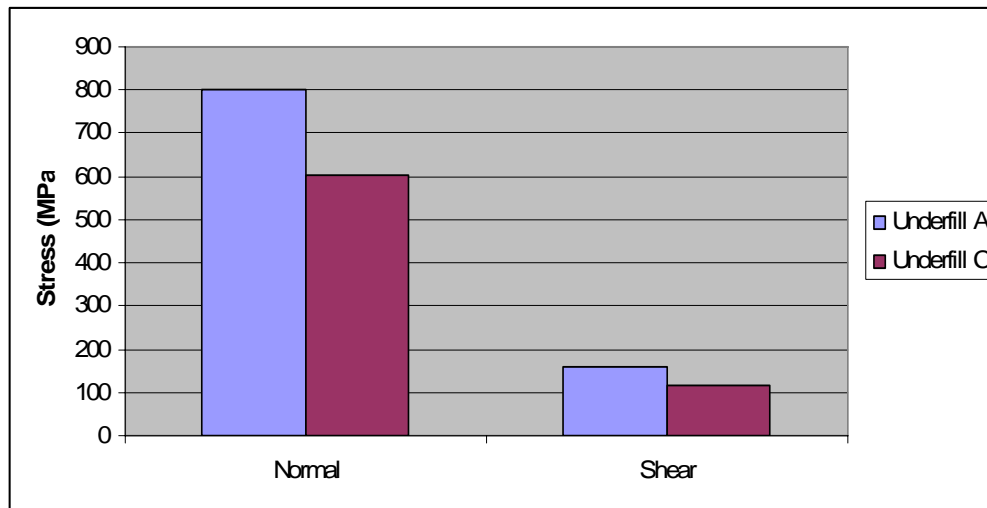


Figure 4.5: Comparison of maximum stress values for the two different underfills

As shown here, the thermal stress in the package with underfill C are less than that in underfill A, which can be attributed to the higher values of thermal co-efficient of expansion for underfill A.

## CHAPTER 5

### COMPARISON WITH PUBLISHED DATA

To establish validity of the analysis done in this work, a comparison is done with published data [3]. In this publication [3] a parametric study is done to study the effect on saturation times, hygroswelling and reflow related stresses on the UBM for different underfill materials, package size etc. The test vehicle chosen is in an 8x8 mm FCBGA package. A schematic of the package is shown below,

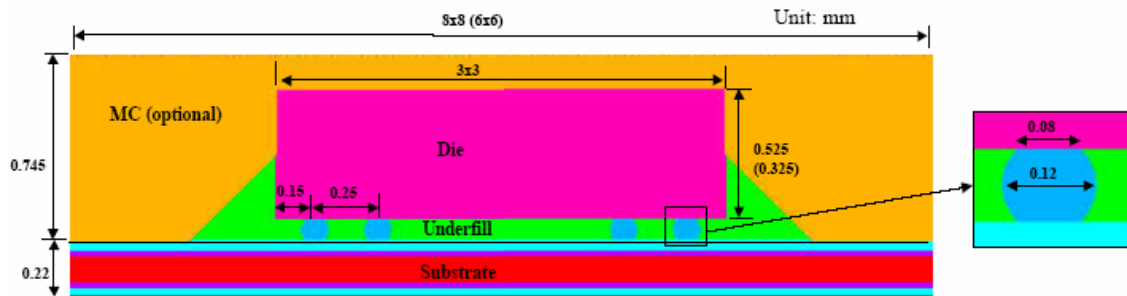


Figure 5.1: Schematic of package

In the present analysis the above package is modeled in ANSYS and the transient moisture diffusion and hygromechanical stress analysis is done for two of the test cases. The test cases chosen are,

1. The control case for the published data, which uses underfill A, has a die thickness of 0.525 mm and a substrate size of 8x8 mm.
2. The same package dimensions but underfill A is replaced by underfill C.



The material property data is provided in the publication and has been used. The Poisson's ratio for the materials is not provided and suitable general values have been assumed for the same.

### 5.1 Modeling

A 2-D half model is constructed for the above package (control case). As in the case of moisture diffusion modeling for the generic package, use of MESH 200 elements is made for die and solder. The same model and mesh geometry is used for both the test cases.

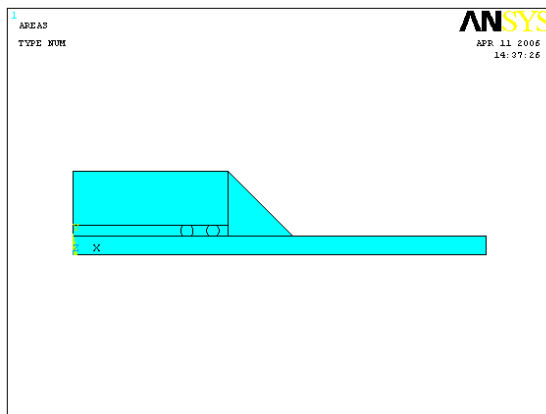


Figure 5.2: FEA model

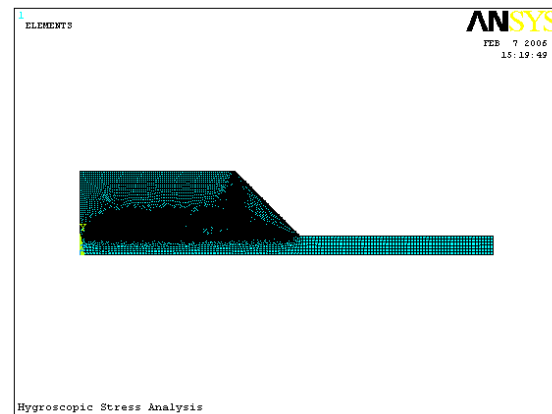


Figure 5.3: Meshed model

Care is taken to make a mesh suitable for both the moisture diffusion and hygroscopic analysis. The solder is so modeled that it has a refined mesh at its sides compared to the remaining part. This is done because the maximum stresses generally occur at these corners as shown earlier. This is also the trend for the present analysis.

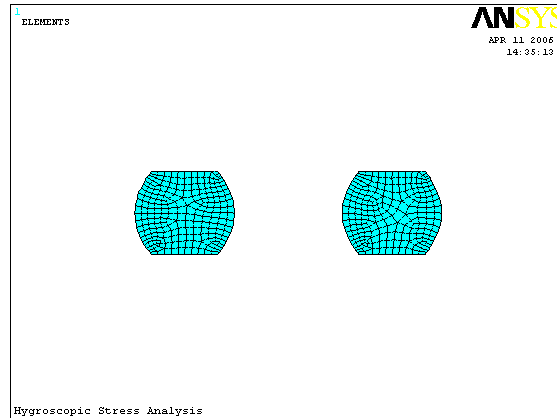


Figure 5.4: Meshed solder balls

### 5.2 Moisture Diffusion Results

The results of the moisture diffusion analysis for the publication [3] are shown below. Here three underfill materials, namely A, B and C are used for parametric study. For the present analysis, the diffusion analysis is done for the underfill materials A and C.

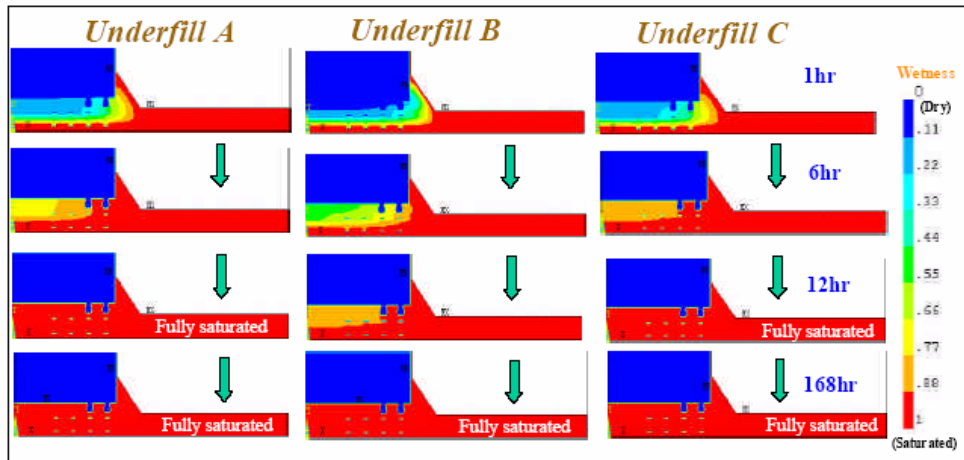


Figure 5.5: Transient moisture distribution for different underfill materials [3]

The moisture distribution for underfill A and C for the present work is shown next.

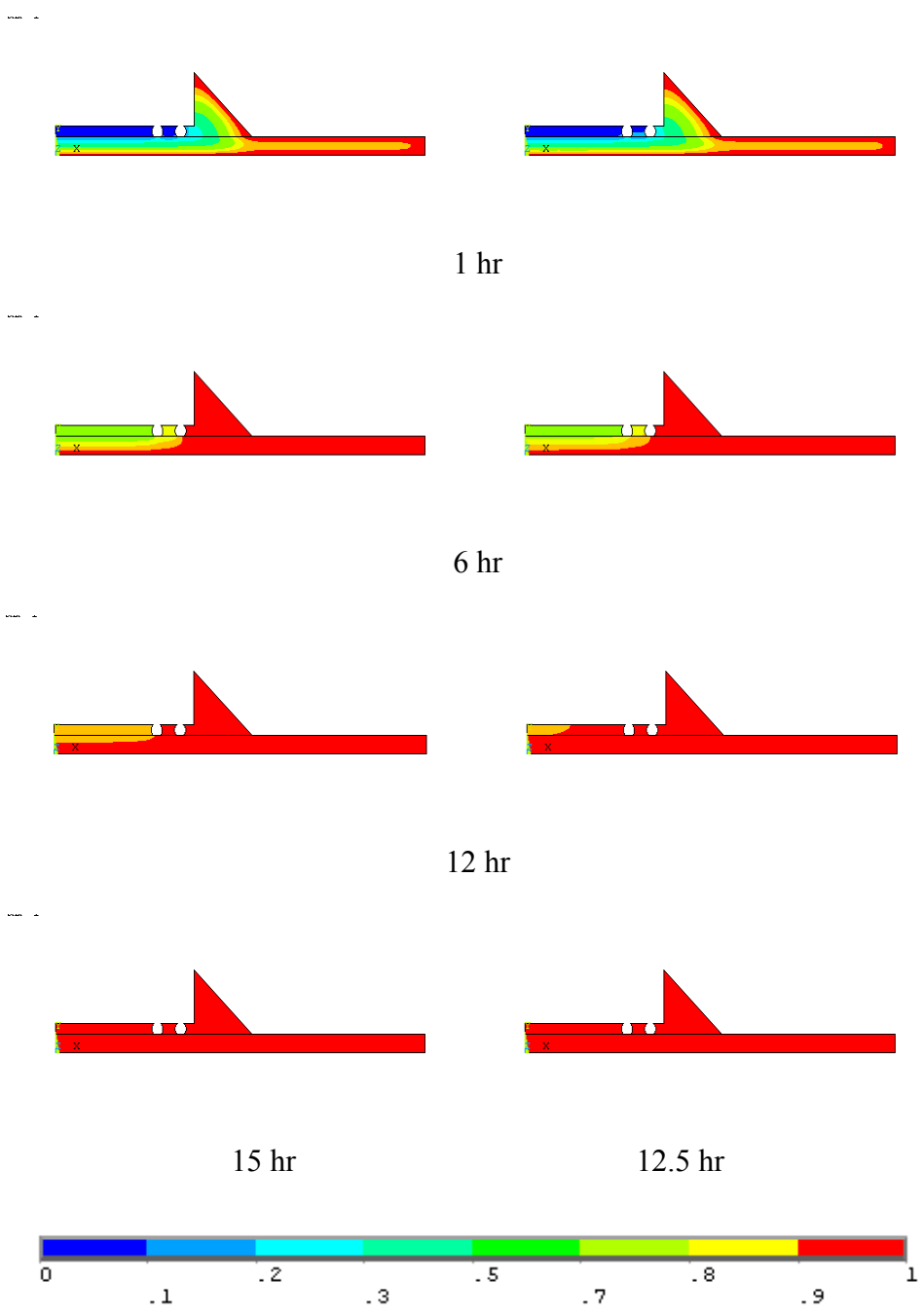


Figure 5.6: Moisture distribution in package with underfill A (left) and underfill C (right)

The saturation is reached in underfill A package in around 15 hours, while the package with underfill C saturates in about 12.5 hours. These values are based on a minimum concentration of around 0.9 in the package. Thus the results for the moisture diffusion are very similar. Also the fact that the package with underfill A takes more time to saturate in the present analysis seems more realistic. This is because the diffusivity of underfill A ( $9.02 \times 10^{-6} \text{ mm}^2/\text{s}$ ) is about 20% less than that of underfill C ( $1.14 \times 10^{-5} \text{ mm}^2/\text{s}$ ).

### 5.3 Hygroscopic Stress Results

In the publication the maximum shear and normal stresses values for the different test cases are plotted in a bar chart. The normal stress ( $S_y$ ) distribution is also shown for the solder with the maximum stresses for the control case.

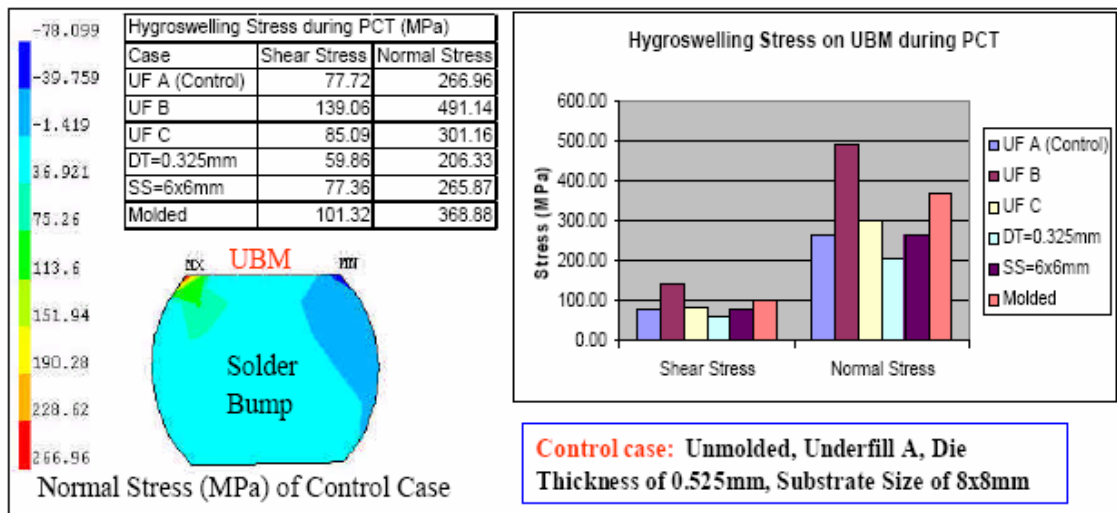


Figure 5.7: Results of parametric studies on hygroswelling stress [3]

In the present analysis, the hygroswelling stresses are computed for the control case and with underfill C. The maximum normal stress acting on the UBM are plotted here.

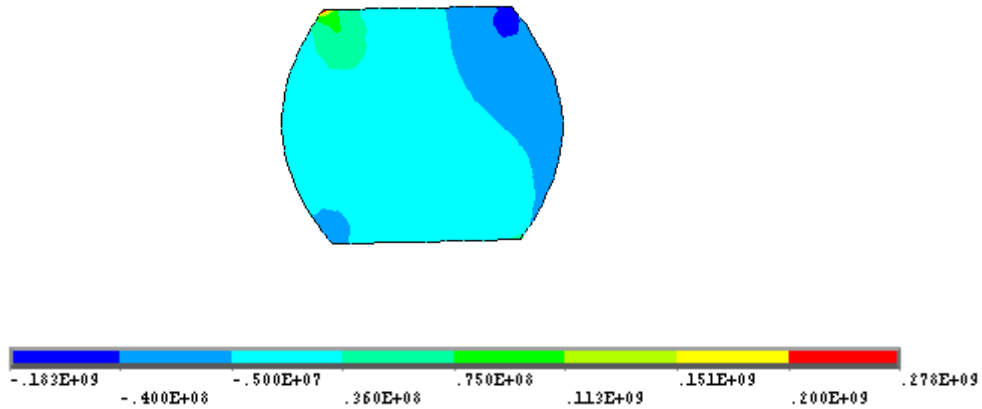


Figure 5.8: Normal stress ( $S_y$ ) distribution in solder with maximum stress (control case)

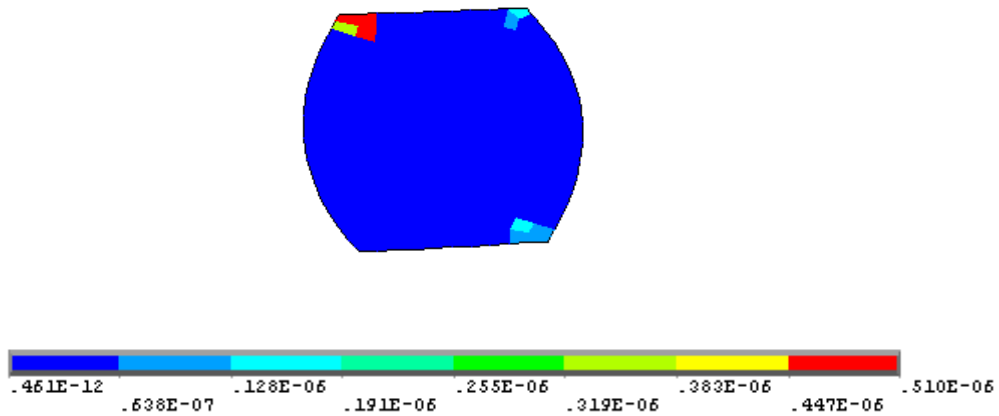


Figure 5.9: Structural energy error estimation for the solder (control case)

A chart is shown next which compares the maximum stress values for the published data and the result from the present analysis for the test cases.

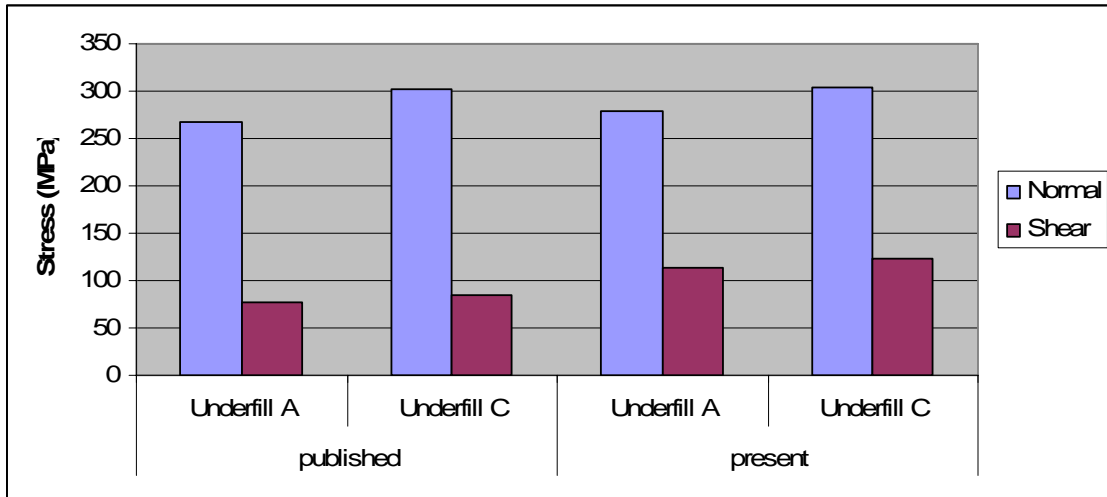


Figure 5.10: Comparison of stress values between published values and present analysis

The results show a close match in the values of the maximum normal stress on the UBM and the normal stress distribution in the solder. It also shows similar patterns of change in stress values with the change in underfill material. However there is a greater mismatch in the values of the maximum shear stress. Possible reasons might be difference in values of Poisson's ratio used for the materials between the present analysis and the published work. Since a plot for the shear stress distribution is not provided in the publication it is difficult to ascertain the degree of mismatch in the distribution of the same.

## CHAPTER 6

### CONCLUSION AND FUTURE WORK

The analyses performed in this work provide an insight on the order and distribution of stresses encountered in FC packages due to hygroswelling and solder reflow. It also illustrates the following points about the moisture diffusion process, the resulting hygroswelling stresses, and the thermal stresses generated in the lead free reflow process

1. The time to saturation of a FC package depends primarily on the diffusivity of its underfill material.
2. The size of a package and the number of solder connections increases the resistance of the package to moisture intake. This is well illustrated from the large difference in saturation times for the generic package and the ones in the published data. [3]
3. The hygroswelling stress primarily depends on the value of the CME of the underfill material. It is also possibly affected by the stiffness of the solder used, with a solder having higher stiffness, like the lead free solder, inducing higher stresses.
4. The thermal stress in the reflow process for lead free solder is higher than the hygroswelling stresses as characterized by material moisture properties at 85 % RH, 85 °C. This is in contrast to the case of using eutectic Pb-Sn solder. [3] The

primary reason for this is the higher peak temperature for the lead free solder case. Also lead free solder in general have a higher Modulus of Elasticity than conventional Pb-Sn solder, which possibly adds to the cause.

### 6.1 Future Work

Quite a few interesting studies can be made on this topic. Some of them are listed below.

1. The measure of moisture saturation time and the resulting hygroscopic stresses for a package of given dimensions and materials but having different layouts of the solder interconnects, like peripheral array or staggered array.
2. The effect of partial under filling on both the thermal stresses during reflow and the hygroswelling stresses. Generally, the thermal performance of the FC package goes down for imperfect under filling. [5, 8] However, the same might possibly reduce the hygroswelling stress and hence the proposed work can be an interesting piece of study.
3. The process of moisture diffusion and resulting hygroscopic stresses can be also be investigated for printed electronics applications, especially those using paper as substrate. This is a challenging work since characterization of moisture properties of the printing inks used might be difficult. However once the moisture properties are determined, the subsequent modeling and analysis will be not very complicated. This is also a rather interesting topic since printed electronic applications are supposed to be greatly in production in recent future.



## APPENDIX A

APDL CODE FOR MOISTURE DIFFUSION (UNDERFILL A)

```

/BATCH
/config, nres, 8000
/COM,ANSYS RELEASE 9.0

!*****
! Moisture Diffusion Modeling
! Polymer: Underfill A
!*****

/GRA,POWER
/GST,ON
/PLO,INFO,3
/COL,PBAK,ON,1,BLACK
/filename,MSD
/TITLE,Moisture Diffusion Simulation
/PREP7

!***** Element types*****
et,1,mesh200,7

et,3,plane77

!***** Material Properties *****

!Temperature in K, Stresses in Pa,

!*****

!Silicon material properties -- #1
!*****
mp,dens,1,1

!Solder material properties -- #2
!*****
mp,dens,2,1

!*****

!FR-4 board material properties -- #3
!*****
mp,dens,3,1
mp,C,3,0.0075e3
mp,kxx,3,0.01597e-9

```

! Underfill Material Properties

!\*\*\*\*\*

mp,dens,10,1

mp,C,10,0.0152e3

mp,kxx,10,0.1374e-9

!\*\*\*\*\* Geometry Model Generation \*\*\*\*\*

nyl=4

nxl=1

tsub=1.0e-3

sbh=150e-6

tdie=0.75e-3

dw=4.323e-3

sw=dw+2.5\*tsub

sbw=58.0e-6

smw=86.0e-6

scc=dw-367e-6

pitch=344.0e-6

\*dim,ylayer,array,nyl

\*dim,xlayer,array,nxl

ylayer(1)=0.0

ylayer(2)=tsub

ylayer(3)=tsub+sbh

ylayer(4)=tsub+sbh+tdie

xlayer(1)=0.0

\*do,j,1,nxl

\*do,i,1,nyl

k,,xlayer(j),ylayer(i)

\*enddo

\*enddo

k,5,sw,ylayer(1)

k,6,sw,ylayer(2)

k,7,dw,ylayer(3)

k,8,dw,ylayer(4)

!Substrate areas  
!\*\*\*\*\*  
a,1,5,6,2

!Silicon areas  
!\*\*\*\*\*  
a,3,7,8,4

!Solder joint area  
!\*\*\*\*\*

k,101,scc-sbw,ylayer(2)  
k,102,scc+sbw,ylayer(2)  
k,103,scc+smw,(ylayer(2)+ylayer(3))/2  
k,104,scc+sbw,ylayer(3)  
k,105,scc-sbw,ylayer(3)  
k,106,scc-smw,(ylayer(2)+ylayer(3))/2

l,101,102  
spline,102,103,104  
l,105,104  
spline,105,106,101

al,9,10,11,12,13,14

agen,12,3,,,-1.\*pitch

!Underfill area  
!\*\*\*\*\*  
l,10,101  
l,12,105  
al,81,14,13,82,17,16  
agen,10,15,,,-1.\*pitch

l,63,70  
l,67,72

al,137,76,77,138,73,74

l,2,3  
l,2,69  
l,3,73  
al,140,139,141,79,80

```
k,,dw,ylayer(2)
l,135,102
l,7,135
l,7,104
al,142,143,144,11,10
```

```
k,,dw+sbh+tdie,ylayer(2)
l,135,8
l,135,136
l,136,8
al,145,146,147
```

```
asel,all
```

```
aglua,all
```

```
!***** Meshing operations *****
```

```
!Solder area
```

```
!*****
```

```
asel,s,area,,3,14
```

```
aatt,2,,1
```

```
*do,i,0,11
```

```
lesize,11+i*6,,8,0.3
```

```
lesize,12+i*6,,16,-3
```

```
lesize,13+i*6,,8,3
```

```
lesize,10+i*6,,8
```

```
lesize,14+i*6,,8
```

```
lesize,9+i*6,,8
```

```
*enddo
```

```
amesh,all
```

```
!Underfill area
```

```
!*****
```

```
asel,s,area,,15
```

```
aatt,10,,3
```

```
lesize,81,(pitch-2*sbw)/8
```

```
lesize,82,(pitch-2*sbw)/8
```

```
amesh,all
```

```
asel,s,area,,30,38
```

```
aatt,10,,3
```

```
*do,i,148,165
    lesize,i,(pitch-2*sbw)/12,-3
*enddo
amesh,all
```

```
!Left End Area of Underfill
!*****
asel,s,area,,26
aatt,10,,3
lesize,140,(pitch-2*sbw)/8
lesize,141,(pitch-2*sbw)/8
lesize,139,sbh/4
amesh,all
```

```
!Right End Area of Underfill
!*****
asel,s,area,,27
aatt,10,,3
lesize,142,(pitch-2*sbw)/8
lesize,144,(pitch-2*sbw)/8
!lesize,143,sbh/4
lesize,143,sbh/8
amesh,all
```

```
!Next Underfill Area from Left End
!*****
asel,s,area,,25
aatt,10,,3
lesize,137,(pitch-2*sbw)/8
lesize,138,(pitch-2*sbw)/8
amesh,all
```

```
!Underfill fillet
!*****
asel,s,area,,29
aatt,10,,3
esize,200e-7
amesh,all
```

```
!Substrate areas
!*****
asel,s,area,,40
aatt,3,,3
esize,600e-7
```

```

amesh,all

!Die areas
!*****
asel,s,area,,39
aatt,1,,1
esize,430e-7
amesh,all

!***** Apply boundary conditions *****

!Boundary conditions for external boundary
!*****
lsel,s,line,,1
lsel,a,line,,2
lsel,a,line,,166
lsel,a,line,,147
dl,all,,temp,1
lsel,all

!***** Solve *****
/solu

antype,4
time,720000 ! 200 hrs
solcontrol,on
nropt,full
lumpm,0
neqit,25
autots,on
nsubst,72000,72000,1000
lnsrch,on
outres,all,-100
kbc,1

!***** Set initial condition *****
tunif,0

solve
finish

save,MSD,db

```

## APPENDIX B

APDL CODE FOR HYGROSWELLING (UNDERFILL A)



```

!*****
!HYGROSCOPIC STRESS MODELLING
!Polymer: Underfill A
!This file is read after the moisture diffusion analysis is done
!*****
/TITLE, Hygroscopic Stress Analysis

/PREP7
!Changing element type from Thermal to Structural
!*****
etchg,tts

!Defining new element type for Solder,Die
!*****
et,2,plane82

!Changing element type
!*****
esel,s,type,,1
emodif,all,type,2
esel,all

!Material Properties for Silicon
!*****
mp,EX,1,155.0e9
mp,alpx,1,0
mp,nuxy,1,0.25

!Material Properties for Solder
!*****
mp,EX,2,45.5e9
mp,alpx,2,0
mp,nuxy,2,0.40

!Material Properties for Substrate
!*****
mp,ex,3,21.0e9
mp,nuxy,3,0.3
mp,alpx,3,0.003 ! ALPX = CME*Csat, CME=0.4

!Material Properties for Underfill
!*****
mp,ex,10,2.4e9
mp,nuxy,10,0.2

```

```
mp,alpx,10,0.0027 ! ALPX = CME*Csat, CME=0.22
```

```
!Deleting all boundary conditions  
!*****  
lsclear,all
```

```
!Applying Boundary conditions  
!*****  
nselect,s,loc,x,0  
dsym,symm,x,0  
nselect,r,loc,y,0  
d,all,uy,0  
nselect,all
```

```
!Apply temperature boundary conditions  
!*****  
! Reading file from msd directory  
!Change to proper directory
```

```
ldread,temp,,,,MSD,rth
```

```
!Solve  
!*****  
/solu
```

```
antype,static,new  
solcon,on,off  
kbc,0  
autots,off  
time,720000  
!nsubst,1000  
nsubst,100  
ncnv,0  
neqit,30  
nropt,full  
lnsrch,on  
outres,all,-10  
save
```

```
!Set initial condition  
!*****  
tunif,0  
solve  
finish
```

## APPENDIX C

### APDL CODE FOR SOLDER REFLOW (UNDERFILL A)

```
/BATCH,LIST
/COM, ANSYS RELEASE 9.0
```

```
!*****
*
!THERMO-MECHANICAL STRESS MODELLING
!Polymer: Underfill A
!*****
*
```

```
/GRA,POWER
/GST,ON
/PLO,INFO,3
/COL,PBAK,ON,1,BLACK
/filename,REFLOW
/TITLE, Thermo-mechanical Stress Analysis
/PREP7
```

```
!***** Element types*****
et,1,plane82
et,2,plane82
et,3,plane82
```

```
!***** Material Properties *****
!Temperature in K, Stresses in Pa, CTE in 1/K, Time in sec
```

```
!Material Properties for Silicon
!*****
mp,EX,1,155e9
mp,alpx,1,2.6e-6
mp,nuxy,1,0.25
```

```
!Material Properties for Solder
!*****
mp,EX,2,42.08e9
mp,nuxy,2,0.40
mp,alpx,2,18.8e-6
```

```
!Material Properties for Substrate
!*****
mp,ex,3,21e9
mp,nuxy,3,0.3
mp,alpx,3,21e-6
```

```

!Material Properties for Underfill
!*****
mp,ex,10,2.4e9
mp,nuxy,10,0.2
mp,alpx,10,145e-6 ! average value

!*****
!**Geometry and Mesh same as for msd.txt hence omitted**
!*****
!Deleting all boundary conditions
!*****
lsclear,all

!Applying Boundary conditions
!*****

!Displacement
!*****
nsel,s,loc,x,0
dsym,symm,x,0
nsel,r,loc,y,0
d,all,uy,0
nsel,all

!Apply temperature boundary conditions
!*****
curetemp = 438 ! in K
tref,curetemp
toffst,0
rampup = 3
rampdown = 5
tempmelt = 220 + 273
tempmax = 255 + 273

time1 = 18
time2 = 80 + time1
time3 = 10 + time2
time4 = 10 + time3
time5 = time4 + 45

!*****

```

```
temp1 = curetemp + rampup*time1
temp2 = temp1
temp3 = temp2 + rampup*10
temp4 = temp3
temp5 = temp3 - 45*rampdown
```

```
!Solve
!*****
/solu
```

```
outres,all
antype,static,new
solcontrol,on,off
autots,off
ncnv,1
neqit,30
nropt,init
lnsrch,on
```

```
!*****
!DUMMY
!*****
deltim,1
tunif,curetemp
time,1e-5
solve
```

```
!*****
!STEP 1 - Ramp up
!*****
esel,all
bfe,all,temp,,temp4
esel,all
```

```
kbc,0
nsubst,5
time,time4
save
solve
finish
```

```
!*****  
!STEP 2 -- Cool down  
!*****  
/delete,REFLOW,rd  
/delete,REFLOW,r001  
/delete,REFLOW,ldhi  
  
/filename,REFLOW  
resume  
  
/solu  
tref,298 ! Room temperature  
kbc,0  
nsubst,5  
antype,,rest  
  
tunif,temp4  
esel,all  
bfe,all,temp,,temp5  
esel,all  
  
time,time5  
save  
solve  
finish  
  
save,REFLOW
```

## REFERENCES

1. Ee Hua Wong ,Yong Chua Teo, Thiam Beng Lim, “Moisture Diffusion and Vapour Pressure Modeling of IC Packaging”, Electronic Components and Technology Conference, pp 1372-1378, 1998.
2. E.H.Wong ,S.W.Koh,K.H.Lee ,R.Rajoo, “Advanced Moisture Diffusion Modeling and Characterisation for Electronic Packaging”, Electronic Components and Technology Conference, 2002
3. Tong Yan Tee, Chek Lim Kho, Daniel Yap, Xavier Baraton, K. Sivakumar, “Comprehensive Moisture Diffusion, Hygroswelling, and Thermo-Mechanical Modeling of FCBGA Package with No-flow Underfill”,APACK 2001 Conference, Singapore, December 2001, pp. 210-216
4. Edwin Bradley and J. Bath, "Lead free project focuses on electronics assemblies," Advanced Packaging, February 2000, pp. 34-42
5. John H. Lau, S-W. Ricky Lee, Chris Chang and Chien Ouyang, “Effects of Underfill Material Properties on the Reliability of Solder Bumped Flip Chip on Board with Imperfect Underfill Encapsulants”, Electronic Components and Technology Conference, 1999
6. R. L. Shook, D. L. Gerlach, and B. T. Vaccaro, “Moisture Blocking Planes and Their Effect on Reflow Performance in Achieving Reliable Pb-free Assembly Capability for PBGAs”, Electronic Components and Technology Conference, 2001



7. R.L.Shook and V.L.Sastry, "Influence of Preheat and Maximum temperature of the Solder-Reflow profile on Moisture Sensitive IC's", Electronic Components and Technology Conference, 1997
8. P. Singh and V. Puligandla, "Failure Modes and Mechanisms in Electronic Packages"
9. [www.semiconfareast.com/flipchipassy.htm](http://www.semiconfareast.com/flipchipassy.htm)
10. [http://www.metallurgy.nist.gov/solder/clech/Sn-Ag-Cu\\_SACAnalysis.htm](http://www.metallurgy.nist.gov/solder/clech/Sn-Ag-Cu_SACAnalysis.htm)
11. Hun Shen Ng a,\*, Tong Yan Tee a, Stephen Pan b, Charles Sun b, and Patrick Lamb, "Development and Application of Lead-free Solder Joint Fatigue Model for CSP", STMicroelectronics
12. Schubert, A., Dudek, R., Auerswald, E., Gollhardt, A., Michel, B., Reichi, H., "Fatigue Life Models of SnAgCu and SnPb Solder Joints Evaluated by Experiments and Simulations," 53rd ECTC Conference Proc., 2003, pp. 603-610.
13. Tong Yan Tee and Hun Shen Ng, "Whole Field Vapor Pressure Modeling of QFN during Reflow with Coupled Hygro-mechanical and Thermo-mechanical Stresses",
14. Peng Su, Sven Rzepka, Matt Korhonen, and C.Y. Li, "The Effects of Underfill on the Reliability of Flip Chip Solder Joints", Journal of Electronic Materials: September 1999
15. Fukuzawa, S. Ishiguro, S. Nambu, "Moisture Resistance Degradation of Plastic LSIs by reflow soldering", Proc. 23<sup>rd</sup> Rel. Phys. Sym., 1985.

16. Wong, E.H., Chan, K.C., Rajoo, R., and Lim, T. B., “The Mechanics and Impact of Hygroscopic Swelling of Polymeric Materials in Electronic Packaging”, Proc. 50th ECTC, 2000, pp. 576-580.
17. Wong, E.H., Chan, K.C., Tee, T.Y., and Rajoo, R., “Comprehensive Treatment of Moisture Induced Failure in IC Packaging”, 3rd IEMT, 1999, pp.176-181.

## BIOGRAPHICAL INFORMATION

Santanu Ghosh completed his Master's in Mechanical Engineering from University of Texas at Arlington in May 2006. He had done his bachelor's from Jadavpur University in India in 2001, followed by more than two years of work in the industry. He is expecting to do a PhD in Mechanical Engineering. His main area of interest is the domain of Thermal Fluids. His present and future research interests include thermo-mechanical aspects of electronic packaging, combustion, and CFD applications in bio-engineering.